OFDM for Data Communication Over Mobile Radio FM Channels—Part I: Analysis and Experimental Results

Eduardo F. Casas, *Member, IEEE,* and Cyril Leung, *Member, IEEE*

Abstract—**This paper describes the performance of OFDM/FM modulation for digital communication over Rayleigh-fading mobile radio channels. The use of orthogonal frequency division multiplexing (OFDM) over mobile radio channels was proposed by Cimini [1]. OFDM transmits blocks of bits in parallel and reduces the bit error rate (BER) by averaging the effects of fading over the bits in the block. OFDM/FM is a modulation technique in which the OFDM baseband signal is used to modulate an FM transmitter. OFDM/FM can be implemented simply and inexpensively by retrofitting existing FM communication systems.**

Expressions are derived for the BER and word error rate (WER) within a block when each subchannel is QAM-modulated. Several numerical methods are developed to evaluate the overall BER and WER. An experimental OFDM/FM system was implemented and tested using unmodified VHF FM radio equipment and a fading channel simulator. The BER and WER results obtained from the hardware measurements agree closely with the numerical results.

I. Introduction

THE demand for data communication over mobile radio channels has increased steadily over the last few years and will likely continue to grow [2], [3]. A common application is found in mobile data terminals (MDT's) used for emergency, law and order, public utility, and a host of commercial services such as courier, dispatch, and inventory control. MDT's allow remote mobile users direct access to computerized databases, resulting in greater productivity. Another benefit is the more efficient use of the allocated (and increasingly scarce) radio spectrum. Features such as the transmission of graphical information or the use of encryption for secure communication can also be readily implemented.

The design of a VHF/UHF mobile radio data communication system presents a challenging problem [4]. In most areas *multipath propagation* causes a moving receiver to experience severe and rapid fluctuations of received signal strength. In a commonly used and proven model [4], [5], it is assumed that there is no line-of-sight path from the transmitter to the receiver; rather, the received signal is made up of a large number of component waves scattered by buildings and other objects near the mobile. Under certain conditions, it can be shown that over short distances the amplitude of the received signal can be well approximated by a Rayleigh distribution. During a deep fade the received signal strength may be reduced to an unacceptably low level. If a conventional serial modulation scheme is used, the bits "hit" by such a fade will be lost.

Recently, Cimini [1] proposed the use of an orthogonal frequency division multiplexing (OFDM) scheme in which the bits in a block (packet) are transmitted in parallel, each at a low baud rate. The intent of the scheme is to spread out the effect of the fade over many bits. Rather than have a few adjacent bits completely destroyed by a fade, the hope is that all the bits will only be slightly affected. Another technique [6] uses a chirp filter to spread individual signaling pulses over time.

The OFDM signal is generated using digital signal processing (DSP) techniques at baseband and this signal must then modulate an RF carrier. In Cimini's [1] proposal the signal is translated directly to the RF frequency, resulting in a system that we call OFDM/SSB. Frequency modulation (FM) can also be used, resulting in our proposed OFDM/FM system. An OFDM/FM system has the advantage that it can use existing unmodified FM radio equipment and can therefore be implemented more quickly and at lower cost than an OFDM/SSB system which requires precise and relatively complex coherent reception.

The following section briefly describes the Rayleigh fading channel and OFDM/FM. A simple model for the OFDM channel is introduced and used to derive the bit and word error rates for OFDM/FM in Section III. Section IV describes several numerical methods that can be used to evaluate the performance of OFDM/FM while Section V describes experimental measurements on an OFDM/FM system and compares the experimental and numerical results.

II. Preliminaries

A. VHF/UHF Mobile Radio Channel

The channel model used in this paper is a nonfrequency-selective (flat) Rayleigh fading model in which additive white Gaussian noise is the major noise source. Field measurements [7]–[12] have shown that the flat fading assumption is reasonable for narrow-band (under 20 kHz bandwidth) signals.

Paper approved by the Editor for Mobile Communications of the IEEE Communications Society. Manuscript received October 5, 1989; revised April 4, 1990. This work was supported in part by a Natural Sciences and Engineering Research Council (NSERC) Post-Graduate Scholarship, Mobile Data International, Inc., Communications Fellowship, and NSERC under Grant A-1731.

The authors are with the Department of Electrical Engineering, University of British Columbia, Vancouver, B.C. V6T 1W5, Canada.

IEEE Log Number 9144542.

0090-6778/91/0500-0783$01.00 © 1991 IEEE

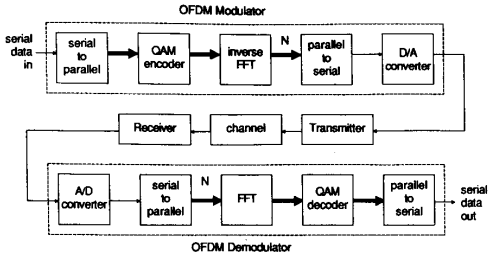

Fig. 1. An implementation of an OFDM system.

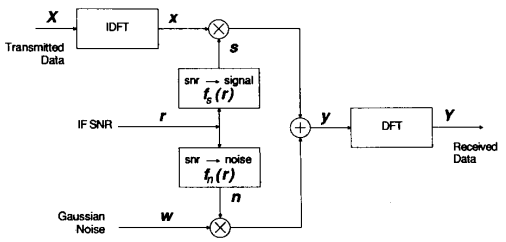

Fig. 2. The equivalent baseband channel model.

B. Orthogonal Frequency Division Multiplexing

Description: OFDM uses frequency division multiplexing with subcarrier frequencies spaced at the symbol (baud) rate. That is, if the block duration is T, the subcarrier frequencies are at $1/T, 2/T, 3/T, \cdots$. This frequency spacing makes the subcarriers orthogonal over one symbol interval [13]–[17]. Modulation is done by using several bits (typically two to five) to set the amplitude and phase of each subcarrier. An OFDM modulator can be efficiently implemented by using an inverse discrete Fourier transform (DFT) to convert the complex phase/amplitude data for each subcarrier into a sampled OFDM signal. Similarly, demodulation can be performed with a DFT which extracts the phase and amplitude of each subcarrier from the sampled OFDM signal.

Because OFDM can be used to efficiently multiplex many bits into one block (symbol), the baud (symbol) rate can be greatly reduced compared to conventional serial modulation methods. The symbol rate is typically reduced by hundreds or thousands of times.

Previously, OFDM modems have been used for data transmission over telephone channels [17]–[21]. OFDM-like multicarrier modems have also been used on HF (3 to 30 MHz) radio channels [22]–[26].

The DFT extracts the phase and amplitude information for $N/2$ (complex) subchannels from the N (real) samples in the block. Some subchannels may not be usable because the signal-to-noise ratio (SNR) at that frequency may be too low. If the fraction of subchannels that are usable is ρ and M bits can be transmitted on each subchannel, then the number of bits per block is $N_b = \rho MN/2$. The block duration is $T = N/f_s$ where f_s is the sampling rate. The bit rate is therefore $R = N_b/T = f_s\rho M/2$.

Implementation: Fig. 1 shows a block diagram of an OFDM implementation. The modulator collects a block of bits from the data source, encodes them into complex (QAM) data values, and converts the data to signal samples using an inverse FFT. The digital-to-analog (D/A) converter produces the analog baseband OFDM signal.

This baseband signal modulates an RF transmitter. The modulated signal is transmitted over the fading channel. A receiver recovers the baseband signal from the received RF signal which may have been corrupted by fading and additive noise.

The demodulator collects a block of samples from the analog-to-digital (A/D) converter, converts the samples to complex data values using an FFT, and decodes the complex data values back into bits.

III. OFDM Bit Error Rate Analysis

In this section, a simple and general model for the mobile radio channel, the *equivalent baseband channel* (EBC) model, is described and then used to obtain an expression for the bit error rate (BER) of OFDM. The assumption that errors occur independently is used to determine the word error rate (WER). The final subsection describes how the EBC model can be applied to the OFDM/FM channel.

A. The Equivalent Baseband Channel Model

The model used to predict the performance of OFDM over mobile radio channels must include all significant effects and yet be kept simple enough for analysis and efficient numerical work. Towards this end, the EBC model converts the effects of fading at IF (or RF) into equivalent effects at baseband. Two effects are considered: time-varying channel gain (fading), and additive noise.

Fig. 2 is a diagram of the EBC model. The received samples, $y = \{y_0, y_1, \cdots, y_{N-1}\}$, are the sum of the received data and noise samples. The received data samples are the transmitted data samples x scaled by the channel gain vector s. The received noise samples are zero-mean Gaussian random variables scaled by the channel noise gain vector n.

Both s and n are functions of r, the IF signal-to-noise ratio (SNR) vector. We assume that the IF noise level is fixed so that r is proportional to the IF signal level. The functions $s = f_s(r)$ and $n = f_n(r)$, define what we call the SN curves of the receiver. The SN curves can be obtained either from analysis of ideal receiver performance [4] or from measurements (Section V).

The model assumes that the receiver SN curves are memoryless. This allows the average signal and noise powers to be obtained by averaging the instantaneous signal and noise powers. Such a quasi-static approximation is valid when the Doppler rate is less than the baseband bandwidth [27], [28], as is the case with land mobile radio applications.

B. BER Analysis

An expression for the BER of a given OFDM block transmitted over the equivalent baseband channel is derived in this section. The notation a indicates a vector $\{a_0, a_1, \cdots, a_{N-1}\}$ and $\langle a \rangle$ denotes the time average of the variable a over N

samples, i.e., $\langle a \rangle = 1/N(a_0 + a_1 + \cdots + a_{N-1})$. The word *sample* is used for quantities in the time domain, while the term *value* is used for quantities in the frequency domain.

Mean and Variance of the Received Value: In Appendix A, the ensemble average of the m-th received data value Y_m over the set of all possible transmitted data vectors with the m-th data value fixed at $X_m = D(D = \pm 1 \pm j)$ and over all possible noise vectors w is found conditioned on a given fixed signal level vector r (and the corresponding s and n) as

$$E[Y_m | X_m = D, X_{-m} = D^*, r] \approx D\langle s \rangle. \tag{1}$$

The conditional variance (given the same conditions as for the mean) of a received data value Y_m, is found to be

$$\mathrm{var}(Y_m | X_m = D, X_{-m} = D^*, r) \approx 2\Big(\langle s^2 \rangle - \langle s \rangle^2 + \langle n^2 \rangle\Big). \tag{2}$$

Bit Error Rate Within a Block: Since the interference (between subchannels) on each subchannel is caused by a large number of independent subchannels, the central limit theorem indicates that the distribution of this interference should be approximately Gaussian. This is confirmed by measurements of the interference distribution in the experimental OFDM/FM system described in Section V. Since the effect of the channel noise is also Gaussian (because of the linearity of the DFT) and independent of the interchannel interference (because r is fixed), the sum of the noise and interference will also be Gaussian and their powers will add.

Using signal-space arguments [29] it is then possible to obtain the BER within a block for the QAM encoding described in Section IV-C as

$$\begin{aligned} \mathrm{BER}_{\mathrm{block}}(\alpha, \beta, \gamma) &= \frac{1}{2} \operatorname{erfc}\left(\frac{\alpha}{\sqrt{2(\beta - \alpha^2 + \gamma)}} \right) \\ &= Q\left(\frac{\alpha}{\sqrt{(\beta - \alpha^2 + \gamma)}} \right) \end{aligned} \tag{3}$$

where $\alpha = \langle s \rangle$, $\beta = \langle s^2 \rangle$, and $\gamma = \langle n^2 \rangle$.

Evaluating the Overall BER: The overall BER can be obtained by using the joint distribution of α, β, and γ, i.e.,

$$\mathrm{BER} = \int_0^\infty \int_0^\infty \int_0^\infty \mathrm{BER}_{\mathrm{block}}(\alpha, \beta, \gamma) p(\alpha, \beta, \gamma)\, d\gamma\, d\beta\, d\alpha. \tag{4}$$

To obtain estimates of the overall BER, the joint distribution of α, β, and γ is required. Unfortunately, no closed-form expression is available for this joint distribution, $p(\alpha, \beta, \gamma)$. In Section IV, a Monte–Carlo numerical integration procedure is described that can be used to evaluate this expression.

C. WER Analysis

In many data communication systems, any error within a related group of bits (a *word*) invalidates all of the bits. In such systems the performance measure of interest is the word error rate (WER). The assumption of random bit errors would simplify the prediction of the error rate of words contained within an OFDM block. Experimental results (see Section V) showed that the independent error assumption is a good approximation for the system that was studied.

In order to predict the WER it will be assumed that the bit errors are independent. Such an assumption would *not* be valid for a conventional serial modulation scheme on a fading channel. With this assumption, the block WER can be expressed easily in terms of the block BER, namely,

$$\mathrm{WER}_{\mathrm{block}} = 1 - (1 - \mathrm{BER}_{\mathrm{block}})^{N_w} \tag{5}$$

where N_w is the number of bits per word.

D. Modeling the OFDM/FM Channel

Baseband Noise Distribution: Although the probability distribution of the FM discriminator output noise depends on the SNR [30], the noise values after the DFT demodulator can be assumed to be Gaussian because the DFT sum makes any noise distribution approximately Gaussian.

Baseband Noise Spectrum: The spectrum of the discriminator noise output also depends on the IF SNR. The distribution of the noise power among the subchannels thus depends on the IF SNR. The distribution of the noise among the different subchannels will vary from block to block because fading causes the IF SNR to vary. To simplify the analysis, however, it was assumed that the blocks were sufficiently long so that the distribution of noise power among the subchannels was almost the same for all blocks. It was also assumed that differences in subchannel SNR's due to the uneven spectral distribution of the noise were corrected by changing the allocation of power among the subchannels in the transmitted baseband signal. The noise spectrum was therefore assumed to be independent of the IF SNR. The validity of this assumption was later verified experimentally.

Experimental measurements of the noise powers in the different subchannels in the presence of fading showed that subchannels at lower frequencies had more noise. This caused subchannels at lower frequencies to have higher error rates. Measurements of the error rates in the different subchannels showed that the error rates could be made approximately equal by using a -10 dB per decade preemphasis at the transmitter in addition to the built-in $+20$ dB per decade standard pre-emphasis.

Random FM Noise: The spectrum of the "random FM" noise at the discriminator output is independent of the SNR and decreases as $(1/f)$ for frequencies above the Doppler rate [27]. The effect of random FM at a given Doppler rate can be included in the model by modifying the 'N' portion of the SN curves. However, this was not necessary since the level of the random FM noise was not significant at any of the Doppler rates measured as shown by the measurements described in Section V-F.

Clipping Noise: Clipping in the FM transmitter was modeled as an additional source of additive white Gaussian noise. Although the clipping is not independent of the signal level, it should normally form a relatively small portion of the total

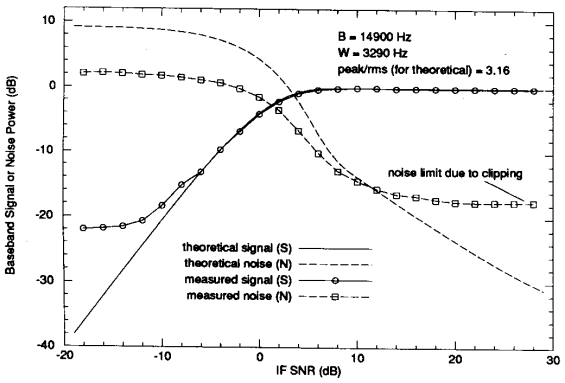

Fig. 3. Theoretical and measured SN curves.

noise power. For example, in the experimental measurements the modulating signal level was set so that clipping distortion had no measurable effect on the BER.

Squelch: Squelch can be incorporated into the SN curves by setting the values of s and n to zero when the IF SNR level falls below the squelch threshold. This assumes an ideal squelch circuit that has no hysteresis or delay.

FM Receiver SN Curves: Fig. 3 shows typical measured and theoretical FM receiver SN curves. This example shows the nonlinear SN curves of an FM discriminator. The measured curves show the effect of baseband SNR limiting due to clipping. The maximum baseband SNR ("limiting baseband SNR") is about 18 dB. A similar effect would be produced by random FM.

IV. Evaluation of Error Rates

This section describes three methods to evaluate the BER and WER performance of OFDM. These are 1) a computation for very short or very long block lengths, 2) a Monte–Carlo integration, and 3) a baseband signal processing simulation. The results obtained using these methods will be compared to experimental results in Section V.

A. BER for Very Short and Very Long Blocks

When the block duration is very short relative to the average fade duration, the received signal level will be constant during the block. Thus, $\langle s \rangle = s$, $\langle s^2 \rangle = s^2$, and $\langle n^2 \rangle = n^2$. The bit error rate for each block, $\mathrm{BER}_{\mathrm{block}}$, as a function of the IF SNR can be averaged over the Rayleigh signal level distribution to obtain the average overall BER. That is,

$$\mathrm{BER}_{\text{short block}} = \int_0^\infty \mathrm{BER}_{\mathrm{block}}\big(s(r), s^2(r), n^2(r)\big)p(r)\,dr. \tag{6}$$

Note that since the signal level is constant over the block $\langle s \rangle^2 = \langle s^2 \rangle$ and (3) simplifies to

$$\mathrm{BER}_{\mathrm{block}}(\alpha, \beta, \gamma) = Q\left(\frac{\alpha}{\sqrt{\gamma}}\right) = Q\left(\frac{s(r)}{n(r)}\right). \tag{7}$$

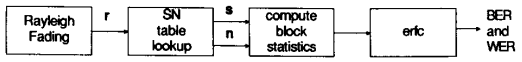

Fig. 4. The numerical integration method.

When the block is very long, each block will have the same statistics and therefore each block will have the same BER. The overall BER will be the block BER for the average block statistics. That is, if

$$\overline{\alpha} = \int_0^\infty s(r)p(r)\,dr, \qquad \overline{\beta} = \int_0^\infty s^2(r)p(r)\,dr,$$
$$\text{and } \overline{\gamma} = \int_0^\infty n^2(r)p(r)\,dr, \tag{8}$$

then

$$\mathrm{BER}_{\text{long block}} = \mathrm{BER}_{\mathrm{block}}\big(\overline{\alpha}, \overline{\beta}, \overline{\gamma}\big). \tag{9}$$

B. Monte–Carlo Integration

The second method uses a Monte–Carlo numerical integration technique to evaluate the BER given by (4). The method involves generating random fading waveforms and then using their α, β, and γ statistics to compute the expected overall BER.

Fig. 4 shows the steps in this procedure. A Monte–Carlo procedure is used in which signal level vectors r are chosen at random from a waveform which is Rayleigh distributed with the appropriate Doppler rate. From each r the values of α, β, and γ and the resulting $\mathrm{BER}_{\mathrm{block}}$ are calculated. The arithmetic mean of these $\mathrm{BER}_{\mathrm{block}}$ values gives the overall BER.

This method can be used to evaluate the BER for any channel that can be accurately described by the EBC model. It is faster than the more detailed simulation described in the following section because it does not involve generating random data or noise or computing DFT's.

C. Software Simulation of the Equivalent Baseband Channel

The OFDM system can be studied in more detail by generating a sampled baseband OFDM waveform and passing it through an equivalent baseband channel. This method involves performing most of the baseband signal processing for an OFDM system. It allows testing of signal processing procedures that cannot be included in the EBC model or whose effect is too complex to analyze. However, this approach is considerably slower[1] than the Monte–Carlo integration method.

Fig. 5 shows the steps involved in the baseband simulation. A block of bits from a pseudo-random bit sequence (PRBS) generator is QAM-encoded into a block of complex values. The inverse FFT generates the baseband OFDM signal by converting each block of $N/2$ complex values into N samples. The Rayleigh-fading generator produces the signal envelope. The SN lookup table and the channel simulator implement the

[1] A typical simulation (about 3 million samples for each of four SNR's and three block sizes) required about 8.5 h CPU time on a Sun 3/50 compared to about 1.5 h for the numerical integration procedure.

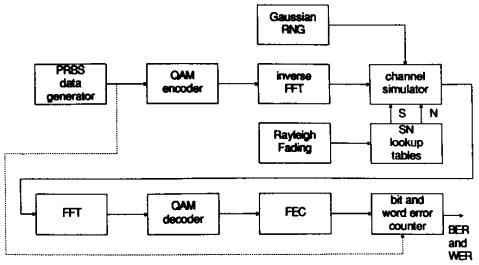

Fig. 5. Simulation using the equivalent baseband channel.

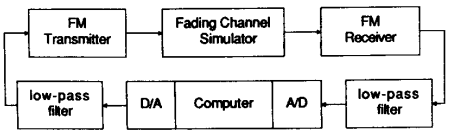

Fig. 6. Block diagram of experimental setup.

equivalent baseband channel (shown in Fig. 2) and combine the baseband signal and Gaussian noise. The FFT demodulates the OFDM signal and the QAM decoder recovers the binary data. The final step in the simulation is to compare the transmitted and received bit sequences and to compute the BER and WER.

The QAM data encoding is done by using two bits per subchannel: one bit for the imaginary (quadrature) component and one bit for the real (in-phase) component. A 0 b is converted to a value of -1, and a 1 b to a $+1$. Unused subchannels are set to zero. The decoding is done by comparing the received values to a threshold of zero.

A more detailed simulation that includes the IF stages of the receiver could be used to study other effects but would require significantly more computation.

V. Experiment

This section describes a laboratory experiment used to demonstrate the feasibility of OFDM/FM using unmodified commercial VHF FM radio equipment. The performance of this experimental system is compared to results obtained using the methods of Section IV.

A. Experimental Hardware

Fig. 6 shows a block diagram of the experimental setup. The various components used are described below. The transmitter and receiver were placed in cast aluminum boxes and their power supply leads were passed through EMI filters to provide RF shielding. An 11 dB 50 ohm attenuator was mounted inside the transmitter shielding box to reduce the RF output level to 12.5 dBm.

Transmitter: The transmitter was an Icom model IC-2AT narrow-band FM transceiver designed for operation in the 144 to 148 MHz amateur band. Its specifications are similar to those of commercial land mobile radio equipment [31]. The audio processing circuitry contains a +20 dB per decade preemphasis network, a limiter (peak clipping) circuit and a low-pass filter. The frequency deviation was measured to be 5 kHz.

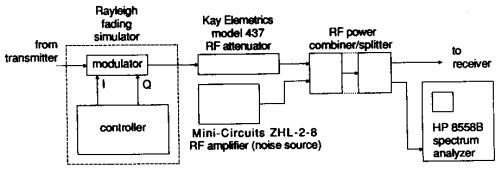

Fig. 7. Fading channel simulator.

Channel Simulator: Fig. 7 shows the channel simulator. The simulator consists of a Rayleigh-fading simulator [32], an RF attenuator, a noise source, and a combiner/splitter.

The signal and noise levels were measured at RF. To ensure that the IF SNR and the RF SNR were equal, the receiver's internal noise was masked by adding noise to the RF signal. The level of noise added ensured that the noise added by the receiver had a small (<0.5 dB) effect on the IF SNR.

Receiver: The FM receiver was another Icom model IC-2AT transceiver. The receiver IF filter bandwidth specification is ± 7.5 kHz at -6 dB and ± 15 kHz at -60 dB. The receiver uses a Motorola MC3357 "Low Power Narrow-Band FM IF" IC for most of the IF and AF signal processing functions. The FM detector is a quadrature-type discriminator [33], [34]. The squelch level was set to minimum so that the receiver audio output was always on.

Computer: An IBM PC/AT-compatible computer was used for all of the digital signal processing tasks as well as test data generation and BER and WER measurement. All of the signal processing computations were done using IEEE-standard 32 b floating point numbers.

A/D and D/A Board: The analog interface circuit was designed and built for this project. It contains a 10 b A/D converter, a 12 b D/A converter, a sample-and-hold amplifier, buffer amplifiers, and a timing circuit.

Reconstruction and Antialiasing Filters: A Krohn–Hite model 3342 filter was used to reconstruct the analog waveform from the D/A output samples. The reconstruction filter used one eighth-order Butterworth low-pass section with a -3 dB frequency of 4 kHz and a one eighth-order Butterworth high-pass section with a -3 dB frequency of 100 Hz. The high-pass section was used to provide AC coupling to the transmitter.

A second Krohn–Hite model 3342 filter was used to low-pass filter the receiver AF output signal to avoid aliasing. This anti-aliasing filter used two cascaded eighth-order Butterworth low-pass sections with -3 dB frequencies of 4 kHz.

Audio Attenuator: An audio attenuator was used to reduce the D/A output (approximately 140 mV rms) to a level suitable for modulating the transmitter (approximately 6 mV rms). The attenuator circuit included a low-pass filter to reduce RF leakage and a switch to turn the transmitter on and off.

B. Experimental Software

The simulation program used in Section IV was modified to make BER and WER measurements over the experimental channel. Instead of using a subroutine that simulates the

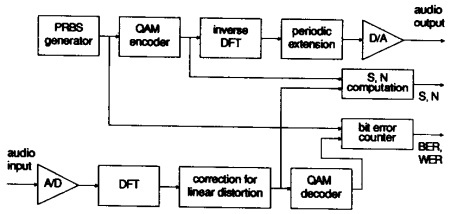

Fig. 8. Signal processing for experimental measurements.

channel, the OFDM signal samples are written to the D/A and read from the A/D. Two additional processing steps were added for use on the hardware channel as follows [35]:

- periodic extension to provide guard times around each block, and
- correction for phase and amplitude (linear) channel distortion.

Fig. 8 shows the signal processing steps for the experimental measurements. A block of pseudorandom bits is QAM-encoded and modulated into a block of OFDM samples. The block of samples is extended to add guard times before and after the block. The samples are sent to the D/A and the resulting analog audio signal modulates the FM transmitter. The recovered baseband (audio) output of the FM receiver is sampled and A/D converted. The received samples are demodulated and the complex data values corrected for the linear distortion effects of the channel. The received complex data values are then decoded into bits which are compared to the transmitted data to compute the BER and WER. The program can also compare the transmitted and received data values on each subchannel to measure the signal and noise powers. This was used to measure the SN curves.

C. Measuring the Baseband SN Characteristics

In order to predict the performance of OFDM over a fading channel, knowledge of the channel's SN curves is required. This section describes the measurement of the SN curves.

The level of the modulating signal will affect the amount of clipping and therefore the SN curves. A reasonable strategy is to set the modulating signal level as high as possible but not so high that distortion due to clipping prevents the system from meeting its BER performance objectives. The modulating signal level was set to give a limiting baseband SNR of 17.5 dB, a level for which the BER was very small[2] ($< 10^{-6}$).

Clipping distortion thus limits the total power of the OFDM modulating signal. This power must be divided among all the subchannels. For the transceivers used in the experiment, the subchannels with the highest SNR's are located around the middle of the baseband frequency range. Determining which subchannels to use involves a compromise between using only the best subchannels to reduce the BER and using more subchannels to increase the bit rate. Brief measurements of BER as a function of E_b/N_0 using various subchannel frequency ranges showed that a reasonable choice was to use frequencies between 1 and 3 kHz and to divide the power equally among the subchannels. An approach that was not tested but is often used [17], [20], [21], [36] is to encode more bits on subchannels with higher SNR's.

SN Curves Measurement Method: The SN curves were measured by transmitting an OFDM signal over the channel and measuring the received baseband signal power and noise power. An OFDM test signal was used for several reasons.

First, the IF filter does not have constant gain across its passband. The power at the input of the discriminator will thus depend on the IF (or RF) spectrum of the FM signal. Therefore, to make SN curve measurements that will apply to OFDM modulation, a signal with same IF spectrum as an OFDM signal is required. Second, the effect of the transmitter's preemphasis filter and the receiver's deemphasis filter will depend on the baseband spectrum of the modulating signal. Third, the effect of the clipping at the transmitter will depend on the probability distribution of the modulating signal. The signal used to measure the SN curves must have the same probability distribution as the OFDM signal in order to properly measure the amount of distortion due to clipping.

There is no crosstalk between subchannels when there is no fading. In this case, the noise received on each subchannel is due solely to additive noise and to distortion effects such as clipping and it is possible to measure the "N" portion of the SN curves.

The simulation program was modified to make SN curve measurements. The signal power (S) was computed as the square of the mean of the received data values. The noise power was computed as the variance (second central moment) of the received data values. The signal and noise powers were measured as an average over the subchannels that were used (1–3 kHz).

SN Curve Results: The measured SN curves are given in Fig. 3 along with those of an ideal discriminator [4]. Each point is an average of 64 1024-sample measurements. The measurements are normalized to give a maximum signal (S) level of 0 dB.

D. BER and WER Measurements

The BER and WER performance of the experimental OFDM/FM system over the nonfrequency-selective Rayleigh-fading channel were measured and compared against results obtained using the numerical techniques.

BER Results: The Doppler rate used in the experimental work and the simulations reported here was 20 Hz, corresponding to a vehicle speed of 25 km/h at a carrier frequency of 850 MHz. The nominal baseband bandwidth was 4 kHz ($f_s = 8$ kHz) and subchannels between 1 and 3 kHz were used ($\rho = 0.5$) with 4 QAM modulation ($M = 2$) giving a bit rate (R) of 4000 bps. The spectrum of the transmitted OFDM/FM RF signal was measured. It was found that the bandwidth is ± 4 kHz at -30 dB, ± 6 kHz at -40 dB, ± 7.5 kHz at -50 dB, and ± 9 kHz at -60 dB.

Blocks of $N = 256$, 1024, and 4096 samples were used corresponding to $N_b = 128$, 512, and 2048 b/block and block durations (T) of 32, 128, and 512 ms, respectively. IF SNR's of 10, 15, 20, and 25 dB were used. The IF bandwidth is

[2]The effect of clipping is different from block to block since the data (and thus the modulating signal) varies.

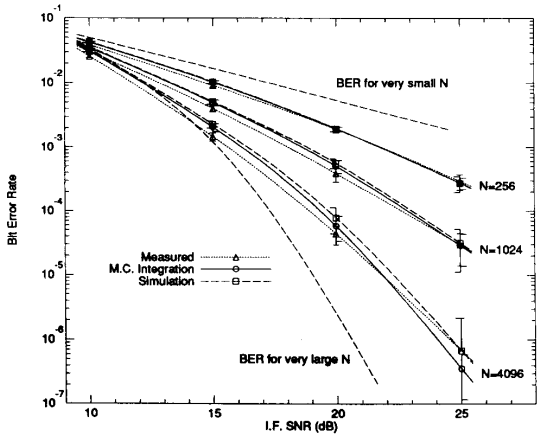

Fig. 9. BER results for $f_d = 20$ Hz and for short and long blocks. The error bars show the 95% confidence intervals. The error bars offset to the right are for the Monte–Carlo (M.C.) integration results, those to the left are for the simulation results, and those that are centered are for the measured results.

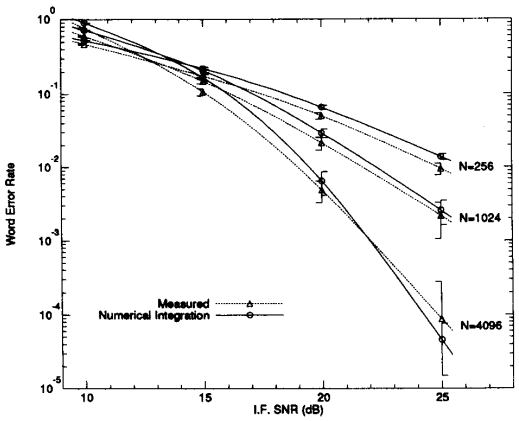

Fig. 10. Measured and computed WER.

14.9 kHz, so that the corresponding values of E_b/N_0 were 16, 21, 26, and 31 dB.

Fig. 9 compares the BER results obtained using 1) the Monte–Carlo integration (Section IV-B), 2) the baseband signal processing simulation (Section IV-C), and 3) the experimental OFDM/FM system. The Monte–Carlo integration and the baseband signal processing simulation used the measured SN curves (Section V-C) shown in Fig. 3. The SN values were interpolated from the measured values over the range from -60 to $+50$ dB in 0.1 dB steps.

The measurements were organized as 12 trials of 60 blocks/trial with 4096 samples/block. For the simulation and the experiment, this represents about 1.5 million bits. For the Monte–Carlo integration this represents a fading waveform duration of about 6 min. As shown by the 95% confidence interval error bars [37], [38], there are large uncertainties at low BER's. The three different BER evaluation methods give results that are within about 1 dB. The BER curves for short and long block lengths (Section IV-A) are shown in Fig. 9.

WER Results: Fig. 10 compares the experimental WER measurements to the predicted WER. The predicted WER was obtained by finding the arithmetic mean of the block WER's computed using (5). The block BER's used in (5) were obtained from the Monte–Carlo integration program. A word length (N_w) of 128 b was used. The two curves agree to within about 1 dB. This indicates that the independent error assumption can be useful in predicting the WER.

The reason why the WER curves for different block lengths intersect in Fig. 10 is as follows. A burst error channel has a lower WER than a random error channel with the same BER because the bit errors tend to be concentrated into fewer words. Making blocks longer (thus putting more words into each block) reduces the variation in the $\mathrm{BER}_{\mathrm{block}}$ from word to word. The bit errors therefore appear to be more random and this results in an increased WER. However, increasing the block length also reduces the BER and this will reduce the WER.

At low SNR's the different block sizes have approximately the same BER as shown in Fig. 9. Thus, at low SNR's using shorter blocks will produce more bursty errors and a lower WER than longer blocks. At high SNR's, the longer blocks have much lower BER's than the shorter blocks and this leads to lower WER's for longer blocks. This explains why the WER curves in Fig. 10 intersect.

E. Effect of Block Duration and Doppler Rate (Tf_d)

The BER performance of OFDM is determined by the time averages of three variables during a block. If the duration of the block is made longer and the fading rate is decreased proportionately, the time statistics of the averages will not change. It would therefore be expected that the OFDM BER performance is determined by the product Tf_d of the block duration T and the Doppler rate f_d. This relationship should hold until the Doppler rate is high enough to produce a significant amount of random FM noise (see Section V-F).

Fig. 11 shows the measured BER performance for Doppler rates of 20 and 80 Hz (100 km/h at 850 MHz) and block sizes of 256, 1024, and 4096 samples. As expected, the BER performance remains almost the same for a given Tf_d product.

F. Random FM

Random FM adds a noise component that increases with the Doppler rate and is independent of the IF SNR. At high Doppler rates the random FM noise power might limit the achievable baseband SNR. Available theoretical analyses of the baseband noise produced by random FM [4], [27] could not be used since they do not take into account the effect of deemphasis.

The average baseband SNR over the 1–3 kHz range at a high (nominally 75 dB) IF SNR was measured while the carrier was fading to see if random FM noise power might have a significant effect. The level of the modulating signal was reduced so that the noise due to random FM could be measured above the noise due to clipping. The modulating signal level

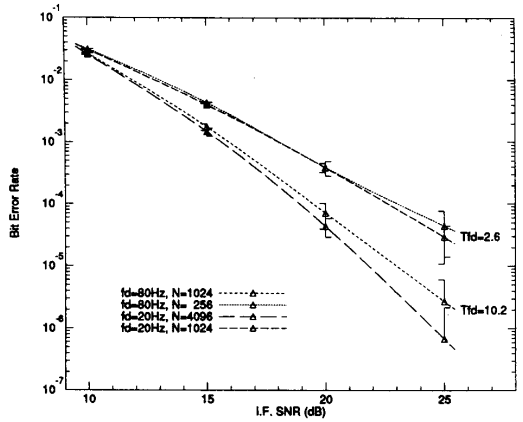

Fig. 11. Measured BER for two values of Tf_d. Lower limits on error bars are not shown if lower limit is off the graph.

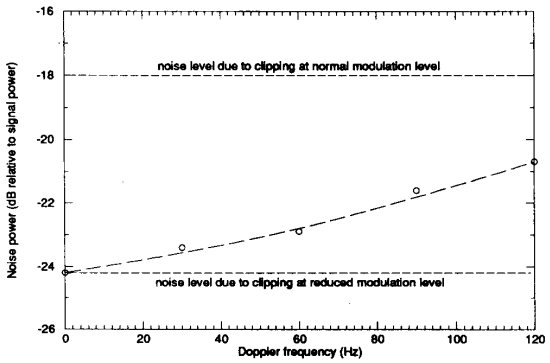

Fig. 12. Random FM and clipping noise power versus Doppler rate.

was reduced by 3.5 dB so that the limiting baseband SNR increased to about 24 dB. Fig. 12 shows the combined clipping and random FM noise power as a function of Doppler rate.

At a Doppler rate of 120 Hz (over 140 km/h at 900 MHz) the random FM noise reduced the baseband SNR to about 20.5 dB. Since the limiting baseband SNR due to clipping during the BER measurements was 17.5 dB, random FM noise should not cause significant performance degradation for 4 QAM subchannel modulation.

VI. Conclusion

A new modulation method, OFDM/FM, has been proposed for data communication over mobile radio channels. OFDM/FM systems can be implemented simply and inexpensively by retrofitting existing FM radio systems.

A simple and versatile model for the mobile radio FM channel, the *equivalent baseband channel* (EBC) model, was developed to study the performance of OFDM/FM. A simple expression was derived for the bit error rate (BER) within a block when each channel is QAM-modulated. An expression was also obtained for the word error rate (WER) by assuming that errors occur randomly within the block. Several numerical methods were developed to evaluate the overall BER and WER. Simple BER expressions were obtained for the cases where blocks are very short or very long relative to the average fade duration. An efficient Monte–Carlo numerical integration method can be used to evaluate the BER and WER for intermediate block lengths. A baseband signal-processing simulation that simulates the effects of fading on the baseband OFDM signal was also written. This allows the study of various coding and signal processing techniques.

An experimental OFDM/FM system was implemented using unmodified commercial VHF FM radio equipment and a fading channel simulator. The BER and WER results obtained from the hardware measurements agreed closely with the results obtained using the numerical methods. This agreement shows that the EBC model can be used to accurately predict the performance of OFDM/FM systems.

A subsequent paper will address several methods for improving the performance of OFDM/FM. These include switching diversity, forward error correction (FEC) coding and a decision feedback correction technique developed for OFDM.

Appendix
The Conditional Mean and Variance of the Error

A.1 Notation

Let a denote the vector $\{a_0, a_1, \cdots, a_{N-1}\}$. The discrete Fourier transform (DFT) of a is defined as $A = \mathrm{DFT}[a]$ where

$$A_m = \sum_{n=0}^{N-1} a_n W^{mn} \tag{10}$$

and the inverse DFT (IDFT) of A is defined as $a = \mathrm{IDFT}[A]$ where

$$a_n = \frac{1}{N} \sum_{n=0}^{N-1} A_m W^{-mn} \tag{11}$$

and

$$W = e^{-j2\pi/N}. \tag{12}$$

The notation $\langle a \rangle$ is used to denote the average of the vector a over N samples, that is,

$$\langle a \rangle = \frac{1}{N} \sum_{i=0}^{N-1} a_i. \tag{13}$$

The notation δ_{ij} is used for

$$\delta_{ij} = \begin{cases} 0 & \text{if } i \neq j \\ 1 & \text{if } i = j \end{cases}. \tag{14}$$

A.2 Assumptions

The received signal y (see Fig. 2) is the sum of received data and noise samples. The received signal samples are the transmitted samples x scaled by the channel signal gain s. The received noise samples are Gaussian random variables w scaled by the channel noise gain n. Both s and n are functions of the RF signal level r which is Rayleigh distributed. The functions $s = f_s(r)$ and $n = f_n(r)$, depend on the type of modulation and the characteristics of the receiver used.

Since the data, signal level, and noise (before fading) are generated by physically independent processes, x, w, and r are assumed to be statistically independent.

It will also be assumed that the spectrum of s is small above a certain frequency. Since the spectrum of r lies below the Doppler rate f_D the spectrum of s will also be concentrated below f_D if the "S" portion of the SN curve is smooth so that there are few nonlinearities in s to produce harmonics.

A.2.1) Data: The transmitted data X is a block of N complex data values, each with energy σ_X^2. For example, for OFDM-QAM $X_m = \pm 1 \pm j$ for all m so that $\sigma_X^2 = 2$. The N real signal samples x which are transmitted over the channel are generated by an inverse DFT (IDFT). For the N samples to be real $X_m = X_{N-m}^*$ (or equivalently $X_m = X_{-m}^*$). This means that only $N/2$ of the complex data values are determined by the data and the remainder are their complex conjugates.

Most practical channels are bandpass channels so that frequencies at the low and high ends of the channel cannot be used. The data values for the unused channels are set to zero at the transmitter. In particular, it is assumed that X_0 and $X_{N/2}$ (both of which have only a real component) are set to zero.

A.2.2) Noise: The N real, i.i.d. (white) noise samples w are taken from a zero-mean Gaussian distribution having a variance σ_w^2.

A.3 Conditional Mean

The ensemble average of the mth received data value Y_m over the set of all possible data vectors with the mth data value fixed at $X_m = D$ (D is complex) and over all possible noise vectors w is found conditioned on a given signal level vector r (and the corresponding s and n). For notational convenience the conditions will often be omitted from the expected value operators although they are implied.

The received signal samples are

$$y_n = s_n x_n + n_n w_n. \tag{15}$$

By using the definition of the DFT, the received value on the mth data subchannel is

$$Y_m = \sum_{n=0}^{N-1} (s_n x_n + n_n w_n) W^{mn}. \tag{16}$$

The conditional mean of the received data values is

$$E[Y_m | X_m = D, X_{-m} = D^*, r] = \sum_{n=0}^{N-1} (E[s_n x_n] + E[n_n w_n]) W^{mn}. \tag{17}$$

Since r (and thus n) is fixed, and the noise w is zero-mean,

$$E[n_n w_n] = n_n E[w_n] = 0. \tag{18}$$

Since s is fixed,

$$E[s_n x_n] = s_n E[x_n]. \tag{19}$$

To evaluate $E[x_n]$ note that since the data values are zero-mean,

$$E[X_k] = D\delta_{km} + D^* \delta_{k(-m)} \tag{20}$$

so that

$$E[x_n] = E\left[\frac{1}{N} \sum_{k=0}^{N-1} X_k W^{-nk}\right] = \frac{1}{N} \sum_{k=0}^{N-1} E[X_k] W^{-nk} = \frac{1}{N} [D W^{-nm} + D^* W^{nm}]. \tag{21}$$

Substituting (18) and (21) in (17),

$$E[Y_m | X_m = D, X_{-m} = D^*, r] = \sum_{n=0}^{N-1} s_n \frac{D}{N} W^{nm-nm} + \sum_{n=0}^{N-1} s_n \frac{D^*}{N} W^{nm+nm} = D \frac{1}{N} \sum_{n=0}^{N-1} s_n + D^* \frac{1}{N} \cdot \sum_{n=0}^{N-1} s_n W^{2nm}. \tag{22}$$

The term $\sum_{n=0}^{N-1} s_n W^{2nm}$ is the DFT of s evaluated at a frequency of twice the subchannel of interest (S_{2m}). If the spectrum of s is concentrated below $m = 2L (S_m \ll S_0$ for $|m| > 2L)$ then for m between L and $N/2 - L$ the contribution of the second term will be small so that

$$E[Y_m | X_m = D, X_{-m} = D^*, r] \approx D\langle s \rangle. \tag{23}$$

A.4 Conditional Variance

The conditional variance (given the same conditions as for the mean) of a received data value Y_m, is

$$\mathrm{var}(Y_m | X_m = D, X_{-m} = D^*, r) = E[Y_m Y_m^*] - |E[Y_m]|^2. \tag{24}$$

Using the definition of the DFT, the first term can be rewritten as

$$E[Y_m Y_m^*] = E\left[\sum_{i=0}^{N-1} \sum_{j=0}^{N-1} (s_i x_i + n_i w_i) \cdot (s_j x_j + n_j w_j)^* W^{mi} W^{-mj}\right]. \tag{25}$$

Using the linearity of the expectation operator, and since x, w, s, and n are real (so that $x_i^* = x_i$, $w_i^* = w_i$, etc.) this can be expanded as

$$E[Y_m Y_m^*] = \sum_{i=0}^{N-1}\sum_{j=0}^{N-1}\big(E[s_i x_i s_j x_j] + E[s_i x_i n_j w_j] + E[n_i w_i s_j x_j] + E[n_i w_i n_j w_j]\big)W^{m(i-j)}. \quad (26)$$

Since s and n are constant because of the conditions

$$E[Y_m Y_m^*] = \sum_{i=0}^{N-1}\sum_{j=0}^{N-1}\big(s_i s_j E[x_i x_j] + s_i n_j E[x_i w_j] + n_i s_j E[w_i x_j] + n_i n_j E[w_i w_j]\big)W^{m(i-j)}. \quad (27)$$

Since the noise is zero-mean ($E[w_i] = E[w_j] = 0$), and w and x are independent,

$$E[x_i w_j] = E[w_i x_j] = 0 \quad (28)$$

so that

$$E[Y_m Y_m^*] = \sum_{i=0}^{N-1}\sum_{j=0}^{N-1}\big(s_i s_j E[x_i x_j] + n_i n_j E[w_i w_j]\big)W^{m(i-j)}. \quad (29)$$

Using the definition of IDFT

$$E[x_i x_j] = \frac{1}{N^2}\sum_{k=0}^{N-1}\sum_{l=0}^{N-1} E[X_k X_l]W^{-ik}W^{-jl}. \quad (30)$$

Using the conditions, and since the data symbols are zero-mean,

$$E[X_k X_l] = \begin{cases} \sigma_X^2 & \text{for } k = -l \\ D^2\delta_{km} + (D^*)^2\delta_{k(-m)} & \text{for } k = l \\ 0 & \text{otherwise} \end{cases} \quad (31)$$

so that

$$\begin{aligned} E[x_i x_j] &= \frac{\sigma_X^2}{N^2}\sum_{k=0}^{N-1} W^{(j-i)k} + \frac{1}{N^2}D^2 W^{-im}W^{-jm} + \frac{1}{N^2}(D^*)^2 W^{im}W^{jm} \\ &= \frac{\sigma_X^2}{N}\delta_{ij} + \frac{1}{N^2}D^2 W^{-m(i+j)} - \frac{1}{N^2}D^2 W^{m(i+j)} \\ &= \frac{\sigma_X^2}{N}\delta_{ij} + \frac{1}{N^2}D^2\big(W^{-m(i+j)} - W^{m(i+j)}\big) \end{aligned} \quad (32)$$

since $D^2 = -(D^*)^2$ for $D = \pm 1 \pm j$.

Since w is real and i.i.d. with zero mean,

$$E[w_i w_j] = \sigma_w^2\delta_{ij}. \quad (33)$$

Substituting (32) and (33) in (29),

$$\begin{aligned} E[Y_m Y_m^*] &= \sum_{i=0}^{N-1}\left(\frac{\sigma_X^2}{N}s_i^2 + \sigma_w^2 n_i^2\right)W^{m(i-i)} + \sum_{i=0}^{N-1}\sum_{j=0}^{N-1} \cdot s_i s_j \frac{1}{N^2}D^2\big(W^{-m(i+j)} - W^{m(i+j)}\big)W^{m(i-j)} \\ &= \sigma_X^2\frac{1}{N}\sum_{i=0}^{N-1}s_i^2 + N\sigma_w^2\frac{1}{N}\sum_{i=0}^{N-1}n_i^2 + \frac{1}{N^2}D^2\sum_{i=0}^{N-1}\sum_{j=0}^{N-1}s_i s_j\big(W^{-2mj} - W^{2mi}\big). \end{aligned} \quad (34)$$

The last term in (34) can be simplified to

$$\begin{aligned} &\frac{1}{N^2}D^2\sum_{i=0}^{N-1}\sum_{j=0}^{N-1}s_i s_j\big(W^{-2mj} - W^{2mi}\big) \\ &= \frac{1}{N}D^2\left(\frac{1}{N}\sum_{i=0}^{N-1}\sum_{j=0}^{N-1}s_i s_j W^{-2mj} - \frac{1}{N}\sum_{i=0}^{N-1}\sum_{j=0}^{N-1}s_i s_j W^{2mi}\right) \\ &= \frac{1}{N}D^2\left(\sum_{j=0}^{N-1}s_j W^{-2mj}\frac{1}{N}\sum_{i=0}^{N-1}s_i - \sum_{i=0}^{N-1}s_i W^{2mi}\frac{1}{N}\sum_{j=0}^{N-1}s_j\right) \\ &= \frac{1}{N}D^2\langle s\rangle\left(\sum_{j=0}^{N-1}s_j W^{-2mj} - \sum_{i=0}^{N-1}s_i W^{2mi}\right). \end{aligned} \quad (35)$$

As in Section A.3, the sums are the DFT's of s evaluated at $\pm 2m$, $S_{\pm 2m}$. Under the same conditions as in Section A.3 the sums ($S_{\pm 2m}$) can be assumed to be negligible compared to $S_0 = N\langle s\rangle$, so that

$$N\langle s\rangle = \sum_{i=0}^{N-1}s_i \gg \sum_{i=0}^{N-1}s_i W^{\pm 2mi}. \quad (36)$$

Using Chebyshev's inequality [39],

$$\frac{1}{N}\sum_{i=0}^{N-1}s_i^2 \geq \langle s\rangle^2, \quad (37)$$

and $|D|^2 = \sigma_X^2$, we find

$$\sigma_X^2\frac{1}{N}\sum_{i=0}^{N-1}s_i^2 \geq |D|^2\langle s\rangle^2 \gg |D|^2\frac{1}{N}\langle s\rangle\sum_{i=0}^{N-1}s_i W^{\pm 2mi}. \quad (38)$$

Thus, from (34)

$$E[Y_m Y_m^*] \approx \sigma_X^2\frac{1}{N}\sum_{i=0}^{N-1}s_i^2 + N\sigma_w^2\frac{1}{N}\sum_{i=0}^{N-1}n_i^2, \quad (39)$$

and the conditional variance of the received data value is

$$\operatorname{var}(Y_m | X_m = D, X_{-m} = D^*, r) \approx \sigma_X^2\langle s^2\rangle + N\sigma_w^2\langle n^2\rangle - |D|^2\langle s\rangle^2. \quad (40)$$

So that the ratio of s and n corresponds to the ratio of the baseband signal and noise, the noise power, σ_w^2, must be

set equal to the baseband signal power σ_x^2. For the case of $D = \pm 1 \pm j$, $\sigma_x^2 = 2/N$ and $\sigma_X^2 = |D|^2 = 2$, we have

$$\mathrm{var}(Y_m | X_m = D, X_{-m} = D^*, r) \approx 2\Big(\langle s^2 \rangle - \langle s \rangle^2 + \langle n^2 \rangle\Big). \tag{41}$$

REFERENCES

[1] L. J. Cimini, "Analysis and simulation of a digital mobile channel using orthogonal frequency division multiplexing," *IEEE Trans. Commun.*, vol. COM-33, pp. 665–675, July 1985.

[2] J. Morris, "MDT's give mobiles direct access to digital computer data bases," *Mobile Radio Technol.*, vol. 1, no. 10, Dec. 1983.

[3] D. C. Cox, "Universal digital portable radio communications," *Proc. IEEE*, vol. 75, pp. 436–477, Apr. 1987.

[4] W. C. Jakes, Ed., *Microwave Mobile Communications.* New York: Wiley, 1974.

[5] R. H. Clarke, "A statistical theory of mobile radio reception," *Bell Syst. Tech. J.*, vol. 47, pp. 957–1000, July 1968.

[6] A. Wittneben, "FMP: A new digital FM scheme with optimized non-coherent detectability and inherent insensitivity to fadings," in *Proc. 39th IEEE Vehic. Technol. Conf.*, San Francisco, CA, May 1–3, 1989, pp. 256–262.

[7] D. Cox and R. P. Leck, "Correlation bandwidth and delay spread multipath propagation statistics for 910 MHz urban radio channels," *IEEE Trans. Commun.*, vol. COM-23, pp. 1271–1280, Nov. 1975.

[8] ——, "Distributions of multipath delay spread and average excess delay for 910-MHz urban mobile radio paths," *IEEE Trans. Antennas Propagat.*, vol. AP-23, pp. 206–213, Mar. 1975.

[9] D. L. Nielson, "Microwave propagation measurements for mobile digital radio application," *IEEE Trans. Vehic. Technol.*, vol. VT-27, pp. 117–132, Aug. 1978.

[10] A. S. Bajwa, "UHF wideband statistical model and simulation of mobile radio multipath propagation effects," *IEE Proc., Part F*, vol. 132, pp. 327–333, Aug. 1985.

[11] G. L. Turin, F. D. Clap, T. L. Johnston, S. B. Fine, and D. Lavry, "A statistical model of urban multipath propagation," *IEEE Trans. Vehic. Technol.*, vol. VT-21, pp. 1–9, Feb. 1972.

[12] H. Hashemi, "Simulation of the urban radio propagation channel," *IEEE Trans. Vehic. Technol.*, vol. VT-28, pp. 213–225, Aug. 1979.

[13] B. R. Saltzberg, "Performance of an efficient parallel data transmission system," *IEEE Trans. Commun. Technol.*, vol. COM-15, pp. 805–811, Dec. 1967.

[14] R. W. Chang, "Synthesis of band-limited orthogonal signals for multichannel data transmission," *Bell Syst. Tech. J.*, vol. 45, pp. 1775–1796, Dec. 1966.

[15] R. W. Chang and R. A. Gibby, "A theoretical study of performance of an orthogonal multiplexing data transmission scheme," *IEEE Trans. Commun. Technol.*, vol. COM-16, pp. 529–540, Aug. 1968.

[16] S. B. Weinstein and P. M. Ebert, "Data transmission by frequency division multiplexing using the discrete Fourier transform," *IEEE Trans. Commun.*, vol. COM-19, pp. 628–634, Oct. 1971.

[17] B. Hirosaki, "A 19.2 kbps voiceband data modem based on orthogonally multiplexed QAM techniques," in *IEEE Int. Conf. Commun.*, Chicago, IL, June 23–26, 1985, pp. 21.1.1–21.1.5 or 661–665.

[18] S. P. Bernard, "A low baud rate 9600 bps voice band modem employing frequency division multiplexing," presented at Workshop on Communications, Commun. Res. Lab. McMaster University, Hamilton, Ont., 1982.

[19] T. Kelly, "Digital modem packs data onto 40 bauds for 9600 bps data comms over voice lines," *Canadian Datasyst.*, vol. 11, pp. 64–65, 67, 69, Apr. 1979.

[20] A. Peled and A. Ruiz, "Frequency domain data transmission using reduced computational complexity algorithms," in *Proc. 1980 IEEE Int. Conf. Acoust., Speech, Signal Processing*, pp. 964–967, 1980.

[21] M. Ballard, "A brief technical overview of the Telebit Trailblazer modem," article posted by R. Siegel, (uunet!telebit!rls) on Usenet, Sept. 1988, Apr. 1988.

[22] A. L. Kirsch, P. R. Gray, and D. W. Hanna Jr., "Field-test results of the AN/GSC-10 (KATHRYN) digital data terminal," *IEEE Trans. Commun. Technol.*, vol. COM-17, pp. 118–128, Apr. 1969.

[23] P. A. Bello, "Selective fading limitations of the KATHRYN modem and some system design considerations," *IEEE Trans. Commun. Technol.*, vol. COM-13, pp. 320–333, Sept. 1965.

[24] R. R. Mosier and R. G. Clabaugh, "Kineplex, a bandwidth-efficient binary transmission system," *AIEE Trans.*, vol. 76, pp. 723–728, Jan. 1958.

[25] D. Kagan and J. M. Perl, "FFT based HF modems performance prediction," in *Proc. IEEE MONTEC'86 (Conf. Antennas Commun.)*, Montreal, P.Q., Canada, Sept. 29–Oct. 1, 1986, pp. 86–89.

[26] J. M. Perl and D. Kagan, "Real-time HF channel parameter estimation," *IEEE Trans. Commun.*, vol. COM-34, pp. 54–58, Jan. 1986.

[27] B. R. Davis, "FM noise with fading channels and diversity," *IEEE Trans. Commun. Technol.*, vol. COM-19, pp. 1189–1200, Dec. 1971.

[28] D. L. Schilling, E. A. Nelson, and K. K. Clarke, "Discriminator response to an FM signal in a fading channel," *IEEE Trans. Commun. Technol.*, vol. COM-15, pp. 252–263, Apr. 1967.

[29] J. M. Wozencraft and I. M. Jacobs, *Principles of Communication Engineering.* New York: Wiley, 1965.

[30] H. Taub and D. L. Schilling, *Principles of Communication Systems.* New York: McGraw-Hill, 1971.

[31] Telecommun. Regulatory Service, Dep. Commun., Government of Canada, "Radio standards specification—Land and mobile stations primarily voice and data modulated FM or PM radiotelephone transmitters and receivers operating in the allocated VHF/UHF bands in the frequency range 27.41 to 866 MHz," Aug. 1985, RSS 119, issue 3.

[32] E. F. Casas and C. Leung, "A simple digital fading simulator for mobile radio," in *Proc. 38th IEEE Vehic. Technol. Conf.*, Philadelphia, PA, June 15–17, 1988, pp. 212–217.

[33] R. Kellejian, *Applied Electronic Communication.* Chicago, IL: Science Research, 1980.

[34] P. Horowitz and W. Hill, *The Art of Electronics.* Cambridge, MA: Cambridge University Press, 1980.

[35] E. F. Casas, *OFDM/FM for Mobile Radio Data Communication.* Ph.D. dissertation, Dep. Elec. Eng., Univ. British Columbia, 1989.

[36] I. Kalet, "The multitone channel," *IEEE Trans. Commun.*, vol. 37, pp. 119–124, Feb. 1989.

[37] P. G. Moore and D. E. Edwards, *Standard Statistical Calculations.* New York: Wiley, 1972, second ed.

[38] I. Miller and J. E. Freund, *Probability and Statistics for Engineers.* Englewood Cliffs, NJ: Prentice-Hall, 1977, 2nd ed.

[39] I. S. Gradshteyn and I. M. Ryzhik, *Table of Integrals, Series and Products.* New York: Academic, 1980.

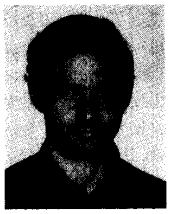

Eduardo F. Casas (S'76–M'90) received the B.A.Sc. degree from the University of Ottawa in 1981, the M.Eng. degree from McMaster University in 1983, and the Ph.D. degree from the University of British Columbia in 1989, all in electrical engineering.

At present he is a Research Fellow with the Electrical and Electronic Engineering Department, University of Adelaide, Australia. His research interests include mobile radio, digital signal processing, and spectral estimation.

Cyril Leung (S'74–M'76) received the B.Sc. (honors) degree from Imperial College, University of London, England, in 1973, and the M.S. and Ph.D. degrees in electrical engineering from Stanford University in 1974 and 1976, respectively.

From 1976 to 1979 he was an Assistant Professor in the Department of Electrical Engineering and Computer Science, Massachusetts Institute of Technology, Cambridge, MA. He was on leave during 1978 at Bell Laboratories, Holmdel, NJ, working on data networks. During 1979–1980 he was with the Department of Systems Engineering and Computing Science, Carleton University, Ottawa, Ont., Canada. Since July 1980, he has been with the Department of Electrical Engineering, University of British Columbia, Vancouver, B.C., Canada, where he is an Associate Professor. In 1987, he was on sabbatical leave at the Department of Electrical Engineering, Ecole Polytechnique de Montreal, Montreal, P.Q., Canada. His current research interests are in mobile radio data communications, coding, and information theory.